

# Electrospun Polyvinyl Alcohol/ Pluronic F127 Blended Nanofibers Containing Titanium Dioxide for Antibacterial Wound Dressing

M. R. El-Aassar<sup>1,2</sup> · G. F. El fawal<sup>2</sup> ·  
Nehal M. El-Deeb<sup>3</sup> · H. Shokry Hassan<sup>4</sup> · Xiumei Mo<sup>1</sup>

Received: 15 October 2015 / Accepted: 15 December 2015 /  
Published online: 21 December 2015  
© Springer Science+Business Media New York 2015

**Abstract** In this study, an antibacterial electrospun nanofibers for wound dressing application was successfully prepared from polyvinyl alcohol (PVA), Pluronic F127 (Plur), polyethyleneimine (PEI) blend solution with titanium dioxide nanoparticles (TiO<sub>2</sub> NPs). PVA–Plur–PEI nanofibers containing various ratios of TiO<sub>2</sub> NPs were obtained. The formation and presence of TiO<sub>2</sub> in the PVA–Plur–PEI/ TiO<sub>2</sub> composite was confirmed by X-ray diffraction (XRD). Transmission electron microscopy (TEM), Fourier transform infrared (FTIR), thermal gravimetric analysis (TGA), mechanical measurement, and antibacterial activity were undertaken in order to characterize the PVA–Plur–PEI/TiO<sub>2</sub> nanofiber morphology and properties. The PVA–Plur–PEI nanofibers had a mean diameter of 220 nm, and PVA–Plur–PEI/ TiO<sub>2</sub> nanofibers had 255 nm. Moreover, the antimicrobial properties of the composite were studied by zone inhibition against Gram-negative bacteria, and the result indicates high antibacterial activity. Results of this antibacterial testing suggest that PVA–Plur–PEI/TiO<sub>2</sub>

---

✉ M. R. El-Aassar  
mohamed\_elaassar@yahoo.com

✉ G. F. El fawal  
gelfawal@gmail.com

<sup>1</sup> Colleges of Chemistry, Chemical Engineering and Biotechnology, Donghua University, Shanghai 201620, China

<sup>2</sup> Polymer Materials Research Department, Advanced Technology and New Material Research Institute, City of Scientific Research and Technological Applications (SRTA-City), New Borg El-Arab City 21934 Alexandria, Egypt

<sup>3</sup> Biopharmaceutical Product Research Department, Genetic Engineering and Biotechnology Research Institute, City of Scientific Researches and Technological Applications (SRTA-City), New Borg El-Arab City, Alexandria 21934, Egypt

<sup>4</sup> Electronic Materials Researches Department, Institute of Advanced Technology and New Material Research Institute, City of Scientific Researches and technological applications (SRTA-City), New Borg El-Arab City, Alexandria 21934, Egypt

nanofiber may be effective in topical antibacterial treatment in wound care; thus, they are very promising in the application of wound dressings.

**Keywords** Nanofibers · Blend · TiO<sub>2</sub> · Antibacterial · Wound dressings

## Introduction

Electrospinning is a simple and relatively low-cost setup for generating nanofibers when compared to advance techniques such as self-assembly processes and phase separation, lithography, and conventional spinning techniques such as melt spinning and wet spinning [1, 2]. Electrospinning has been applied to generate diverse nanofibers for various applications such as filters, skin masks, semi-permeable membrane, clothing, and medical materials [3, 4]. Recently, nanofibers have been applied towards medical uses such as drug delivery systems, tissue engineering scaffolds, vascular grafts, biological wound dressings, and support for the human body [5–7]. Electrospun nanofibers exhibit several unique special properties such as surface area, high porosity network, extremely lightweight, and design flexibility for specific physical/chemical surface functionalization [1, 8]. Nanofibers with antibacterial functionality can be produced by incorporating antibiotics or effective antibacterial agents in the fabricated matrix via electrospinning. As a polymer bioactive matrix, natural or synthetic polymer types are often chosen for the electrospinning. These antibacterial agents give rise to many favorable properties of nanofibers mat that are having and will have a wide range of biomedical applications such as wound dressing [9–13]. Additionally, nanofibers have a high capacity for loading of biological substances and active materials such as silver or titanium dioxide nanoparticles [14, 15]. Polyvinyl alcohol (PVA) deserves a special attention because of its good environmental stability, a hydrophilic synthetic polymer, and easy processability. Besides, it is one of the frequently investigated hydrogel of electrospun fibers including the application to biomedical applications due to its remarkable properties, such as non-toxic polymer, biodegradable, elasticity, complexing ability, and biocompatibility as well as mechanical properties [16, 17]. Since PVA was discovered, the applications of PVP have increased tremendously; PVA undergoes crosslinking and lead to the formation of PVA hydrogel having excellent transparency and anti-electrostatic properties. It has been used as a main component of temporary skin covers or wound dressing. However, a major drawback for deployment of PVA in aqueous media is its high degree of swelling and solubility. So, a series of PVA hydrogels prepared by PVA cross linking blends play a significant role as biomedical materials [18–20]. Poly (ethylene oxide)–poly (propylene oxide)–poly(ethylene oxide) (PEO–PPO–PEO) triblock copolymer, commercially available as Poloxamer or Pluronic. Pluronic are the commercial names that find widespread industrial applications as emulsifying, wetting, thickening, coating, solubilizing, stabilizing, dispersing, lubricating, and foaming agents [21–25]. Since the PEO segment of Pluronic is highly hydrophilic, Pluronic has been widely investigated in biomedical and cosmetic applications for reducing protein adsorption and cell adhesion. Polyethyleneimine (PEI), a cationic polymer, molecule may exist in a linear or branched form. Branched PEI is a polyamine with a high positive charge density that allows adsorbing tightly onto negatively charged substrates. PEI has a wide range of

uses, as a flocculating agent for wastewater treatment, an ink upgrading agent to improve dispersion and adhesion force, and an electroplating bath additive to improve product's gloss and smoothness just to name a few. PEI is also extensively used in biological applications [26, 27]. As a strongly cationic polymer, it can bind to certain proteins. It is used as a marker in immunology and also used to precipitate and purify enzymes and lipids. One of the most important nanomaterials which has attracted a great attention due to its unique properties is titanium dioxide ( $\text{TiO}_2$ ).  $\text{TiO}_2$  is also widely used as a food and pharmaceutical additive, as well as white pigment in the paper industry and in cosmetic products. Nanoparticles of  $\text{TiO}_2$  are used in cosmetics, filters that exhibit strong germicidal properties and remove odors, and in conjunction with silver as an antimicrobial agent. It is considered non-toxic and has been approved by the American Food and Drug Administration (FDA) for use in human food, drugs, cosmetics, and food contact materials [28]. The nanoparticles provide a slow release of titanium ions that have wound-healing and antimicrobial properties. The titanium ions released from nanoparticle inhibits microbial proliferation, and hence, it accelerates wound healing [29]. In the present study, electrospun PVA-Plur-PEI blended nanofibers containing  $\text{TiO}_2$  nanoparticles are proposed to be used as antibacterial dressings.  $\text{TiO}_2$  nanoparticles with mean sizes of 4–20 nm were successfully prepared by the sol–gel methods. These nanoparticles have great promise as antimicrobial agents. Electrospun blended nanofibers containing various ratios of  $\text{TiO}_2$  nanoparticles were obtained. The structure of the blended nanofibers containing  $\text{TiO}_2$  was characterized, and the mechanical properties were measured. Moreover, the antibacterial test results showed that PVA-Plur-PEI/  $\text{TiO}_2$  nanofibers have better bactericidal activity than the PVA-Plur-PEI nanofibers against Gram-negative bacteria.

## Materials and Methods

### Materials

Polyvinyl alcohol (PVA) was supplied by Fluka, Switzerland; Polyethyleneimine (PEI) (low Mw, 50 % solution in water, Mn 1.800 (GPC); typical Mw 2.000), Pluronic® F-127(Plur), titanium (IV) isopropoxide (TTIP), and all the chemicals were purchased from Sigma-Aldrich Chemicals Ltd. (Germany). Distilled water was used as the solvent to prepare hydrogel samples. All other chemicals and analytical reagent were analytically graded and used without any further purification.

### Preparation of $\text{TiO}_2$ NPs

In order to produce sol–gel-derived  $\text{TiO}_2$  NPs, precursor material titanium IV isopropoxide (TTIP) was used. Isopropanol was used to dissolve the precursor to obtain homogenous solution of the precursor as a solvent. The precursor solution was prepared by dissolving 1 ml of titanium IV isopropoxide in 32 ml of isopropanol with vigorous stirring for 30 min forming white solution. Yellow precipitation was formed by dropwise addition of citric acid (0.05 g dissolved in 4 ml distilled water) with vigorous stirring for 120 min at 60 °C. Finally,  $\text{TiO}_2$  NPs powder was filtered off, washed with distilled water and ethanol three times, and dried in vacuum at 60 °C (overnight) to give the resulting composites of nano- $\text{TiO}_2$ . Finally,

the dry powder was eventually purified using a muffle at 500 °C for 5 min to obtain TiO<sub>2</sub> nano-single crystals.

### Preparation of PVA–Plur–PEI/ TiO<sub>2</sub> NPs Blend Solutions

The homogenous hydrogel solutions of PVA, Plur, and PEI for spinning were prepared in water by simultaneously dissolving PVA (7.5 wt%) at 50 °C, and then 0.5 g Plur were added and stirred for about 60 min till the solution became homogeneous. PVA/Plur solutions were prepared by mixing in five blending ratios (7.5/0.5), (7/1), (6.5/1.5), (6/2), and (4/4) wt% for about 60 min. After that, 200 µl of PEI solution (50 % solution in H<sub>2</sub>O) was gradually dropped into the above solution; the mixture was stirred for about 60 min. Finally, addition of TiO<sub>2</sub> NPs in concentrations 0.01, 0.03, and 0.05 wt% were mixed with the selected polymer blend with stirring overnight to make composite of PVA–Plur–PEI/TiO<sub>2</sub> NPs.

### Electrospinning of PVA–Plur–PEI/ TiO<sub>2</sub> Blend Nanofibers

The prepared blend with the TiO<sub>2</sub> NPs were loaded into a glass syringe with a metal capillary needle (inner diameter=0.5 mm). The electrospinning setup (Inovenso NE100, Turkey) consisted of a syringe pump and a grounded collector plate covered in aluminum foil, and a high voltage power supply was applied to the PVA–Plur–PEI/ TiO<sub>2</sub> NPs blend solution in a syringe via an alligator clip attached to the syringe needle. The electrospinning were performed at room temperature, and the solutions were injected from the syringe pump with a feed rate of 1.3 mL/h. The distance between the needle tip and the grounded collector plate was 17 cm, and the high voltage was applied at 23 kV. Dry nanofibers were collected directly from the aluminum foil and stored at room temperature.

### Characterization of the Formed Membranes

#### *Transmission Electron Microscopy*

The surface morphologies of TiO<sub>2</sub> NPs, PVA–Plur- PEI blend nanofibers, and PVA–Plur–PEI/ TiO<sub>2</sub> NPs blend nanofibers were carried out using a transmission electron microscope (TEM, JEOL JEM-2100, Japan) at acceleration voltage of 15 kV. Samples were splattered with gold before observed. Scanning electron micrographs were evaluated using Image J software. At least 100 isolated nanofibers were randomly selected, and their diameters and diameter distributions were measured and averaged. And the average particle size of TiO<sub>2</sub> NPs was determined by measuring the particle size from the TEM micrographs using SMILE VIEW SOFTWARE developed by JOEL.

#### *Fourier Transform Infrared Spectroscopy*

The chemical structure of blend nanofibers was studied with Fourier transform infrared spectroscopy (FTIR) spectra. All spectrum were taken at room temperature using FTIR spectrometer (Shimadzu FTIR-8400 S, Japan), with spectral a range of 4000–400 cm<sup>-1</sup>.

### *X-ray Diffraction*

To confirm the crystalline structure of the TiO<sub>2</sub> NPs in the PVA–Plur–PEI blend nanofibers, X-ray diffraction (XRD) patterns were recorded with TiO<sub>2</sub> NPs using an X-ray power diffraction (Shimadzu XRD 7000 X-ray diffractometer, Japan) at a voltage of 30 kV and a current of 30 mA with Cu K $\alpha$  radiation ( $\lambda=0.15418$  nm) in a  $2\theta$  range from 10° to 80°. The measurement was repeated three times.

### *Thermo Gravimetric Analysis*

The thermo gravimetric analysis was carried on a Thermo Gravimetric Analyzer (Shimadzu Thermal Gravimetric Analysis (TGA)—50, Japan). The TGA trace was obtained in the range 20–600° C under nitrogen atmosphere with a flow rate of 20 mL/min and at a heating rate of 10 C/min. The graph was plotted with weight (mg) vs. temperatures.

### *Tensile Strength and % Elongation at Break*

The mechanical properties of PVA–Plur–PEI and PVA–Plur–PEI/TiO<sub>2</sub> NPs blend nanofibers were characterized using a tensile tester (model AG-I, Shimadzu, Japan) according to ASTM ID: D882-12. Specimens with 6 mm  $\times$  1 mm dimensions were cut and used for analysis at a crosshead speed of 30 mm/min. The specimen thicknesses were measured using a digital micrometer (Mituto, Tokyo, Japan), having a precision of 0.001 mm. Sheets strips were fixed between the grips, and the crosshead speed was set at 30 mm/min. The average values from five repetitions were taken as the tensile strength and strain at break results.

### **Neutral Red Assay for Toxicity**

Cytotoxic assay was performed according to Borenfreund and Puerner, 1985, in order to draw a broad line about the safety degree of the used agent [30]. Briefly, by using fibro blast cells, cell suspension of  $6 \times 10^4$  cell/ml was collected and seeded in 96-well plates. The plates were incubated at 37 C in humidified 5 % CO<sub>2</sub> for 24 h, and the exhausted old medium was discarded and replaced by the prepared nanofibers with RPMI medium or RPMI medium only (as a negative control). The cell plates were incubated at the same growth conditions for 3 days. After 3 days, the exhausted culture medium was discarded, and 100  $\mu$ l of neutral red stain (100  $\mu$ g/ml) was added to each well and incubated for 3 h at 37 C in humidified 5 % CO<sub>2</sub>. Only living cells are permeable to neutral red and incorporated it into liposomes providing a quantitative assay to the cytotoxic effects. Excessive dyes were discarded, and the stained cells were fixed with 100  $\mu$ l fixing solution (0.5 % formalin with 1 % CaCl<sub>2</sub>) for 1 min; then cells were destained in 100  $\mu$ l destaining solution (50 % ethanol with 1 % acetic acid glacial) for 5 min by shaking. The stain intensity was assayed using automated ELIZA (BINDER BIOTECK E LX 800) microplate reader adjusted at 540 nm (reference filters 620 nm) to calculate the cytotoxicity percentages of the membranes on the cells.

### **Antibacterial Activity of Blend Nanofibers on Resistant Bacteria**

The susceptibility of the resistant bacterial growth to membrane nanofibers was evaluated by a microplate reader assay [31]. The purified and identified clinical isolates of Gram negative like

*Pseudomonas aeruginosa* (*P. aeruginosa*), *Salmonella typhi* (*S. typhi*), and *Escherichia coli* (*E. coli*) were kindly provided by the microbiological lab of Mabaret Alasafra hospital, Alexandria, Egypt with its identification report. Briefly, aliquot of 500  $\mu\text{l}$  of preinoculated bacterial strains (104 CFU/ml) in lysogeny broth (LB) media. LB was transferred to each well of 6-well plates. A cubic part of each membrane (1 cm  $\times$  1 cm; pre-sterilized with UV for 2 h) or 500  $\mu\text{l}$  of LB broth were added to each well in replica. The plates were incubated at 37  $^{\circ}\text{C}$  for 24 h. After incubation, the absorbances of the plates were determined using automated ELIZA microplate reader adjusted at 620 nm.

The inhibition percentage of PVA–Plur–PEI/TiO<sub>2</sub> nanofibers was calculated according to the following equation:

$$\text{Inhibition percentage} = \frac{A-A1}{A0} \times 100$$

Where A is the absorbance of the treated group, A1 is the absorbance of the blank, and A0 is the absorbance of the control group.

## Results and Discussion

### Characterization of TiO<sub>2</sub> NPs

Figure 1 shows the surface morphology and the average particle size of TiO<sub>2</sub> nanoparticles prepared by sol–gel method using a transmission electron microscope (TEM). From the Fig. 1, it is visibly judged that the particle is in nanostructure with spherical morphology of the prepared powder. The images indicated that TiO<sub>2</sub> NPs, with uniform particles of size appearing at  $\sim 6$  ( $\pm 10$ ) nm with a porous morphology, which confirmed the small nanoparticles formed via the sol–gel methods.

The crystalline phase of TiO<sub>2</sub> NPs was determined by the X-ray diffraction method (XRD). The XRD patterns of TiO<sub>2</sub> NPs are shown in Fig. 2. XRD patterns exhibited strong diffraction

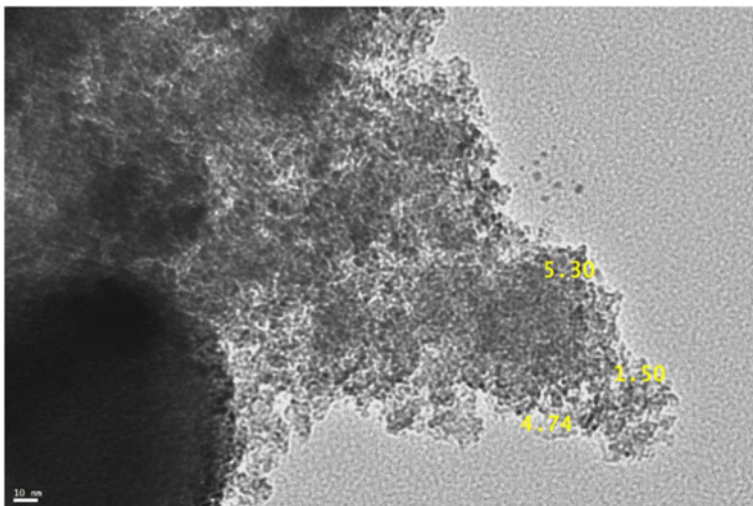


**Fig. 1** TEM micrographs of dried TiO<sub>2</sub> NPs, bar scale: 10 nm



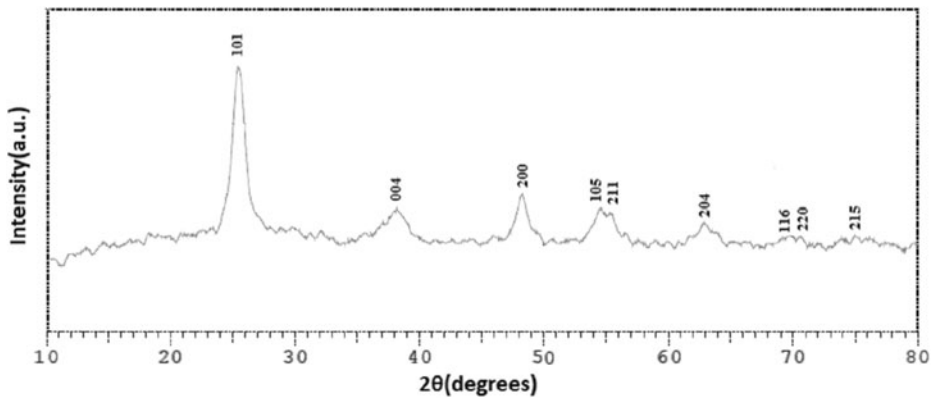


**Fig. 2** X-ray diffraction (XRD) patterns of TiO<sub>2</sub> NPs

peaks at  $2\theta=25.4^\circ$  (101),  $38^\circ$  (004),  $48^\circ$  (200) and  $55^\circ$  (211), indicating TiO<sub>2</sub> NPs in the anatase phase (JCPDS 78–2846), and no peaks of impurities are detected. From the sharp peaks, it is obvious that the obtained TiO<sub>2</sub> NPs have high crystallinity, and it is confirmed by the (1 0 1) crystalline peak [32, 33].

### Morphological Characterization of Nanofibers

The effects of the different concentration of Plur on the solution properties of PVA–Plur–PEI blends and on the morphology of the resultant nanofibers were studied using a scanning electron microscope (SEM). PVA–Plur–PEI solutions were maintained at a total concentration of 8 wt%. The surface morphology of electrospun nanofibers are presented in Fig. 3a–e. According to the SEM images, the surface morphology and the average diameter of the blend nanofibers are dependent on initially added Plur concentrations. We find that increasing Plur ratio in the PVA–Plur–PEI blends showed beaded nanofibers (Fig. 3a, d).

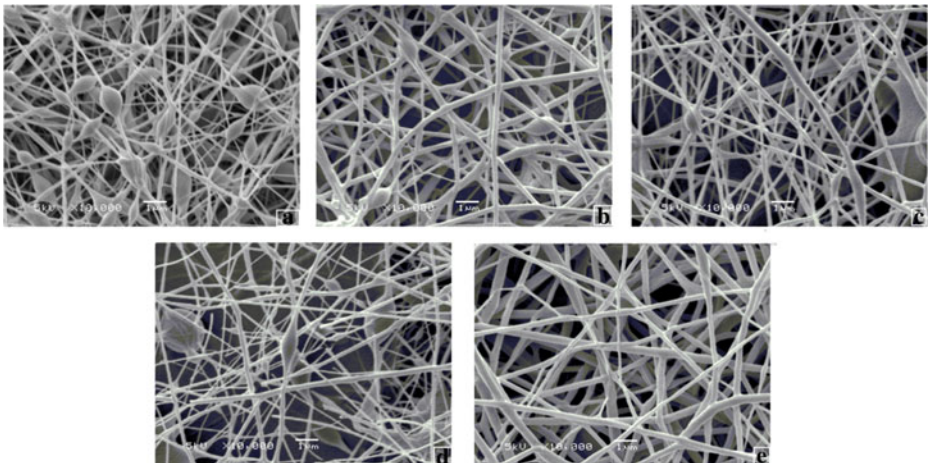


**Fig. 3** SEM images of nanofiber with various blend ratios (PVA: Plur) **a** 4:4, **b** 6:2, **c** 6.5:1.5, **d** 7:1, and **e** 7.5:0.5

The beads in fibers occurred when the content of Plur in the blended solution increased to 50 wt%, and the number of beads decreased with decreasing the concentration of Plur. However, when concentration of Plur was lower than 1 wt% generates the morphology of nanofibers was uniform and bead free Fig. 3e. The capillary breaking of the electrospun jets by surface tension led to the formation of the beaded nanofibers. A similar result was previously reported by Shalumon et al. [34].

Figure 4 shows SEM morphology and diameter distribution of PVA–Plur–PEI blend nanofibers with/without 0.01 % TiO<sub>2</sub> NPs under the same processing condition (total concentration, 8 wt %; blend ratios (7.5 PVA, 0.05 Plur) voltage, 23 kv and distance 17 cm). Addition of TiO<sub>2</sub> NPs did not show any effect on the morphology (beadless and smooth) nanofibers was obtained (Fig. 4a, b), but the addition of TiO<sub>2</sub> NPs to the blend solution affect on the average diameter and distribution of the nanofibers, the average diameter decreased from 280 ± 20 nm for PVA–Plur–PEI blend nanofibers to 130 ± 20 nm for of PVA–Plur–PEI/0.01 % TiO<sub>2</sub> nanofibers (Fig. 4a, b). Moreover, the distribution of the PVA–Plur–PEI blend nanofiber became broader. This behavior mainly attributed to the charge density increases in the PVA–Plur–PEI/ 0.01 % TiO<sub>2</sub> blend solutions during electrospinning, resulting in strong electrostatic repulsion among the sprays. This repulsive force easily overcomes the surface tension of the jet to reduce diameters of the nanofibers [35]. So, the final diameter size of the PVA–Plur–PEI/0.01 % TiO<sub>2</sub> NPs becomes smaller.

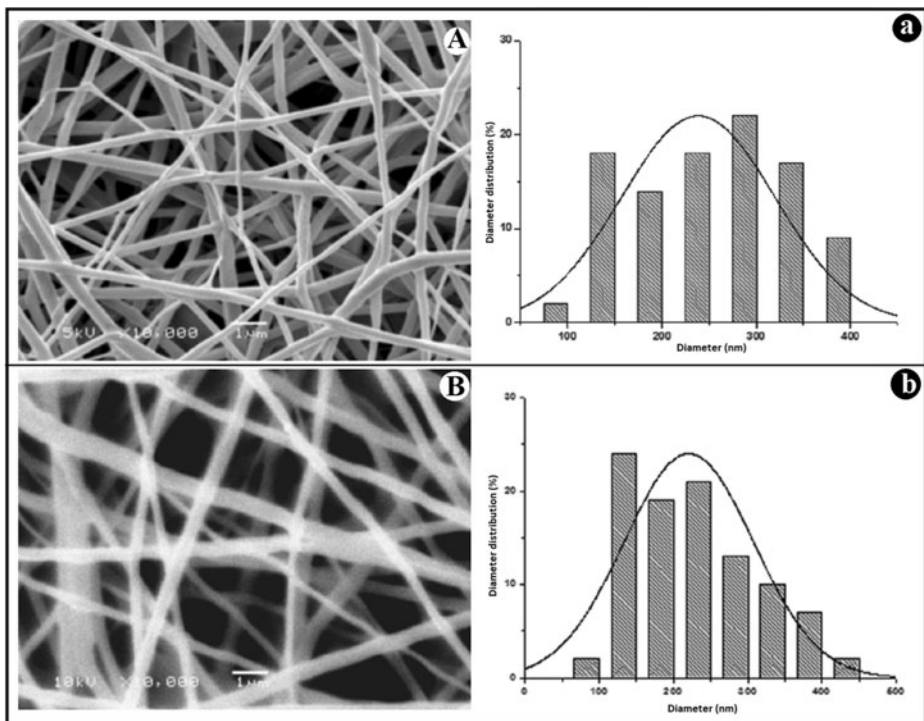


**Fig. 4** SEM images and distribution of the average diameter of **A, a** PVA–Plur–PEI, and **B, b** PVA–Plur–PEI/0.01 TiO<sub>2</sub> NPs



## Mechanical Properties

The mechanical properties of nanofibers of PVA- Plur-PEI/TiO<sub>2</sub> blend nanofibers were determined from the stress–strain curves and listed in (Fig. 5). The stress and strain with different TiO<sub>2</sub> concentrations show the same trend. The tensile strength of the PVA–Plur–PEI blend nanofibers increases with the concentration of TiO<sub>2</sub> NPs increasing to 0.03 wt%, which indicates that incorporating the presence of TiO<sub>2</sub> NPs leads to an enhancement of the blend nanofibers, and the introduction of the TiO<sub>2</sub> NPs may reinforce the crystallinity of PVA–Plur–PEI blend [36]. However, tensile strength at higher concentration of TiO<sub>2</sub> NPs (0.05 wt) was reduced. This may be attributed to increasing agglomeration of TiO<sub>2</sub> particles at the higher concentration, which could act as stress concentrations, leading to premature breaking.

## FTIR Data

FTIR spectra data was carried out for the surface characterization of the individual components, as well as surface structure of PVA–Plur–PEI, and PVA–Plur–PEI/TiO<sub>2</sub> NPs blend nanofibers are shown in Fig. 6. In Fig. 6a, the pure PVA nanofibers exhibited characteristic absorption bands at 2924 and 3430 cm<sup>-1</sup> associated with a C–H stretching broad and –OH group, respectively. Additionally, the characteristic absorption bands at 1110 cm<sup>-1</sup> (the stretching vibration of C–O–C) and 2934 cm<sup>-1</sup> show the main functional groups of Plu (Fig. 6b). The PVA–Plur–PEI blend nanofibers (Fig. 6c, d) shows additional peaks at 1640 cm<sup>-1</sup>, and there were also bands at 3410 cm<sup>-1</sup> which characterize that the amino peak was stronger. Furthermore, the spectra also showed a–CH– of stretching vibration absorption peak are 2940 cm<sup>-1</sup>, which indicated successful incorporation of the different components.

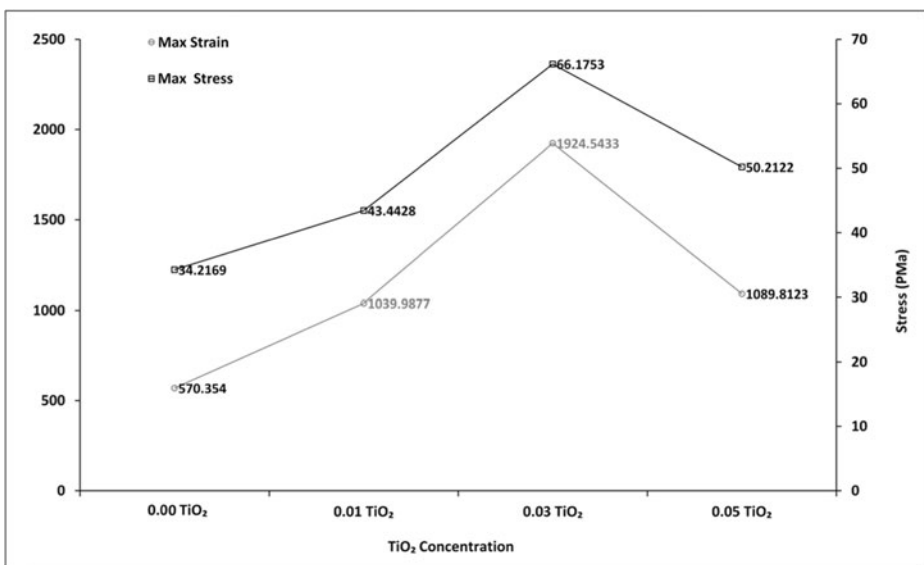


**Fig. 5** The stress and strain of PVA–Plur–PEI/ TiO<sub>2</sub> at various content of TiO<sub>2</sub> NPs

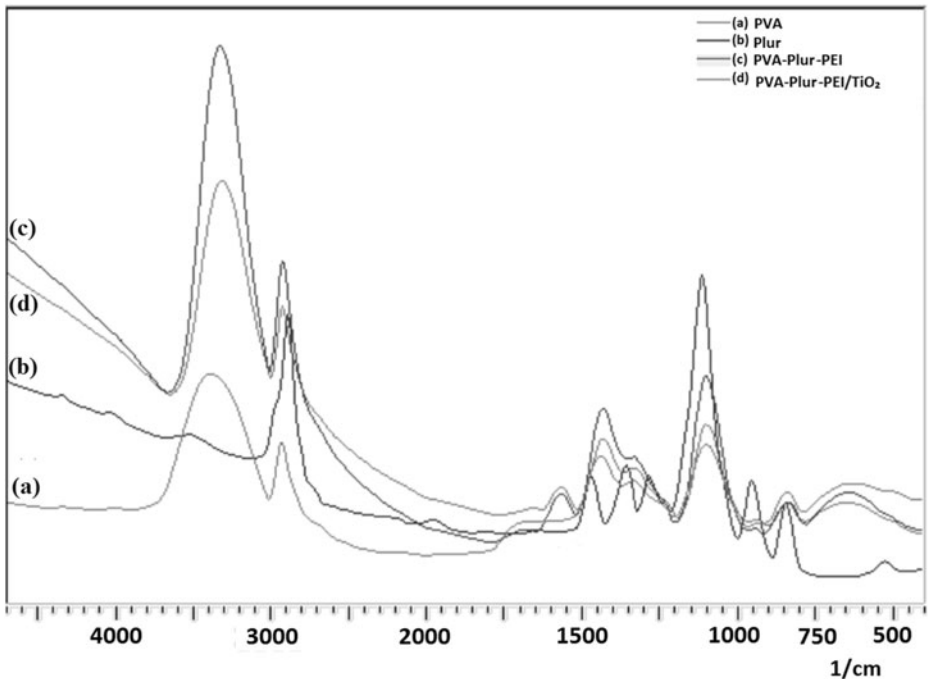


**Fig. 6** FTIR spectra of **a** PVA, **b** Plur, **c** PVA–Plur–PEI, and **d** PVA–Plur–PEI/ TiO<sub>2</sub> NPs electrospun nanofibers

## Thermal Properties

The thermal degradation behavior of the control PVA, and Plur components, PVA–Plur–PEI blend, and PVA–Plur–PEI blend nanofibers containing 0.01, 0.03, and 0.05 wt% TiO<sub>2</sub> NPs were studied by means of TGA. Figure 7 displays the thermal degradation behavior of PVA has shown the third stage of weight loss at 250–350 °C, 350–450 °C, and 450–520 °C followed by a final decomposition of the polymer that begins around 580 °C. For the Plur sample, the initial decomposition temperature is about 230 °C. The second step was in a temperature range of 240–410 °C. The thermal decomposition temperature of composite PVA–Plur–PEI blend nanofibers, and PVA–Plur–PEI blend nanofibers containing TiO<sub>2</sub> NPs at the same trend of thermal stability. The higher thermal stability might be attributed to the main chain and final structure of the blend polymer and its additional contents of TiO<sub>2</sub> NPs to the nanofiber membrane.

## Cytotoxicity of Nanofibers Containing TiO<sub>2</sub> NPs

Toxicokinetics described the entering rates of certain substances to the body through different exposure routes and its fate after its entering (Fig. 8). These processes may occur after exposure through inhalation, ingestion, dermal contact, and intraperitoneal or intravenous injection. TiO<sub>2</sub> NPs and PVA dermal adsorption gains great interest because TiO<sub>2</sub> NPs could be included in many consumer products such as cosmetics and sunscreens [37], in addition to the biomedical application of PVA membranes as wound dressings [38].

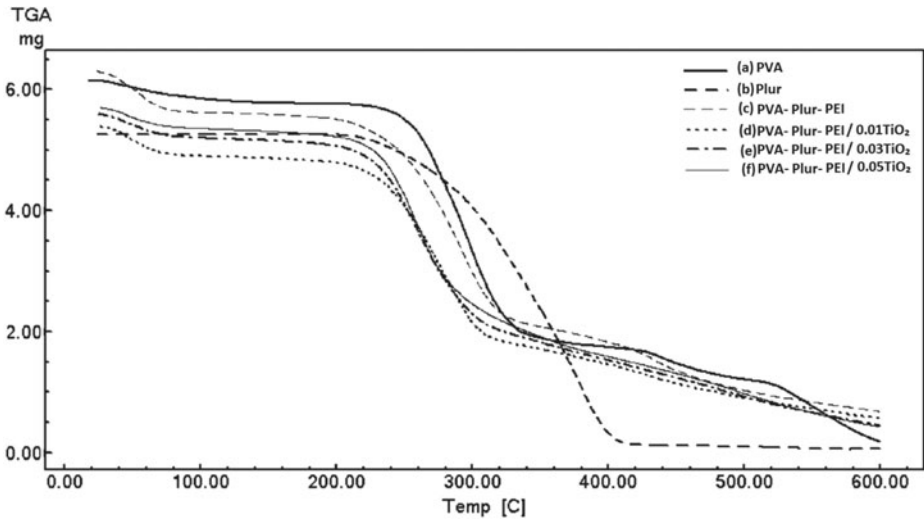


**Fig. 7** TGA of **a** PVA, **b** Plur, **c** PVA–Plur–PEI, **d** PVA–Plur–PEI/ 0.01 TiO<sub>2</sub> NPs, **e** PVA–Plur–PEI/0.03 TiO<sub>2</sub> NPs, and **f** PVA–Plur–PEI/ 0.05 TiO<sub>2</sub> NPs electrospun nanofibers

This current study will be the first report that explains how TiO<sub>2</sub> NPs alter the possible toxicity of PVA–Plur–PEI blend on fibroblast cells, promoting cell death, as demonstrated by the neutral red assay. Our results clarified that the decrease in the measured absorbance levels along the time reflects the absence of fibroblast cellular proliferative capability in the presence of PVA–Plur–PEI blend. In addition, TiO<sub>2</sub> NPs showed a great capability to reduce the toxicity

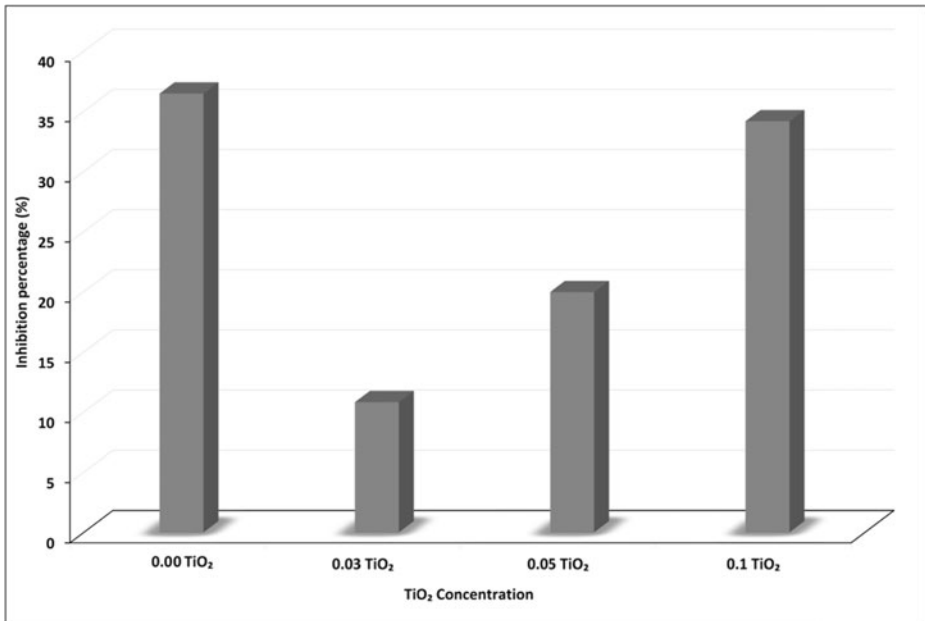


**Fig. 8** Cytotoxicity assay of TiO<sub>2</sub> NPs on the cells

of PVA–Plur–PEI blend (0.00 TiO<sub>2</sub>) from 36.4 to 10.8 % when the prepared membrane treated with 0.01 % TiO<sub>2</sub> NPs. On the same hand, one closely correlated article describes the same concept but through the blended of PVA with chitosan [39]. This report explained that fibroblast cell on PVA/chitosan blended membrane has better spreading and growth than on PVA membrane alone. To that end and among the many pharmaceutical used aspects of nanotechnology in the dermatology field, the antimicrobial action of TiO<sub>2</sub> metal oxide nanoparticles with their potential application as therapeutic agents has great attention [40].

### Antibacterial Activity of Nanofibers Containing TiO<sub>2</sub> NPs

The antibacterial results of the prepared polymers against *P. aeruginosa*, *S. typhi*, and *E. coli* were shown in Fig. 9. The concluded data revealed that generally, PVA–Plu–PEI nanofibers containing maximum concentration of TiO<sub>2</sub> NPs does not showed the maximum inhibition of all bacterial growth. Among all pathogenic bacterial strains, *P. aeruginosa* was the most resistant strain to the used polymers. The maximum inhibition percentage in *P. aeruginosa* growth (21.63) was recorded with PVA–Plur–PEI nanofibers containing TiO<sub>2</sub> NPs (0.03 %) with a slightly different value with the control nanofibers (20.6). In contrast, *E. coli* was the most sensitive strain that exhibited 53.88 % inhibition in bacterial growth upon the treatment with PVA–Plur–PEI nanofibers containing TiO<sub>2</sub> NPs (0.01 %). On the other hand, the maximum inhibition percentage in *S. typhi* growth was obtained upon the treatment with PVA–Plur–PEI nanofibers containing TiO<sub>2</sub> NPs (0.03 %); 44.7. In the current study, PVA–Plur–PEI nanofibers containing TiO<sub>2</sub> NPs showed a maximum ability to inhibit the growth of the resistant *E. coli* with inhibition percentage 53.5 comparing with PVA–Plur–PEI nanofibers that recorded 28.4. The antimicrobial of TiO<sub>2</sub> NPs which are highly efficient in inhibiting the bacterial growth are now available commercially [41]. Nanoparticles with antimicrobial properties provided many pharmacological advantages in reducing acute toxicity, overcoming resistance and lowering cost, over conventional antibiotics uses [42]. Up to 2010, it was

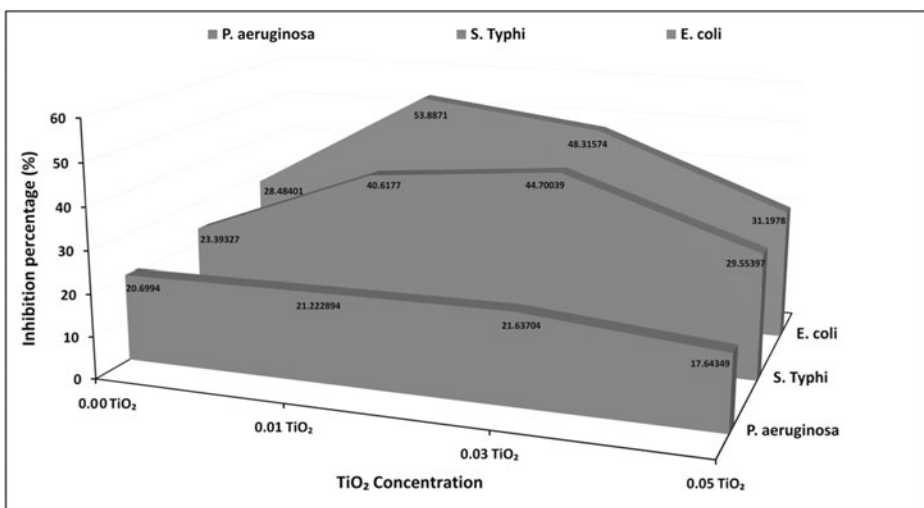


**Fig. 9** Diameter inhibition zone (cm) of electrospun nanofibers against *Pseudomonas aeruginosa* (*P. aeruginosa*), *Salmonella typhi* (*S. typhi*) and *Escherichia coli* (*E. coli*)

reported that TiO<sub>2</sub> NPs failed to exhibit antibacterial activity alone, [43] but recently, Vincent et al. (2014) demonstrated that TiO<sub>2</sub> NPs without any kind of combination inhibited the pseudomonas growth [44]. Also, Santhoshkumar et al. (2015) [45] stated that the synthesized TiO<sub>2</sub> NPs showed antibacterial activity against *Staphylococcus aureus* (25 mm) and *E. coli* (23 mm). Finally, we could concluded that PVA-Plur-PEI/ TiO<sub>2</sub> NPs nanofibers could be used as a good wound dressing membrane in addition, the blended of PVA-Plur-PEI/ TiO<sub>2</sub> NPs nanofibers improved the membrane safety levels on human fibroblast cells and the antimicrobial activity against the resistant pathogens.

## Conclusion

In this work, TiO<sub>2</sub> NPs with mean sizes of 4–20 nm were successfully synthesized by the sol-gel methods and characterized. PVA-Plur-PEI blend nanofibers with varying ratios of Plu, and PVA-Plur-PEI blend nanofibers with 0.01, 0.03, and 0.05 % TiO<sub>2</sub> NPs concentrations were successfully fabricated by electrospinning technique. It is found that the surface morphology and the average diameter of the blend nanofibers are dependent on initially added Plur concentrations. Also, the fiber diameter of the blend nanofibers were gradually decreased due to the addition of TiO<sub>2</sub> NPs. the antimicrobial properties of the PVA-Plur-PEI/ TiO<sub>2</sub> nanofibers have better bactericidal activity than the PVA-Plur-PEI nanofibers against Gram-negative bacteria. This nanofiber from PVA-Plur-PEI/ TiO<sub>2</sub> could be promising approach for enhanced wound treatment, skin infection treatments, and tissue regeneration.

**Acknowledgments** This work was supported by postdoc Programs Foundation of Ministry of Education of China Grant No is (2015 M57145)

## References

1. Ramakrishna, S., Fujihara, K., Teo, W., Lim, T., & Ma, Z. (2005). *An introduction to electrospinning and nanofibers* (pp. 135–137). Singapore: World Scientific Publishing Co. Pte, Ltd.
2. Wendorff, J. H., Agarwal, S., & Greiner, A. (2012). *Electrospinning: materials, in: processing, and applications*. Germany: Wiley-VCH.
3. Fouda, M. G., El-Aassar, M. R., & Al-Deyab, S. S. (2013). Antimicrobial activity of carboxymethyl chitosan/polyethylene oxide nanofibers embedded silver nanoparticles. *Carbohydrate Polymers*, *92*, 1012–1017.
4. Greiner, A., & Wendorff, J. H. (2007). Electrospinning: a fascinating method for the preparation of ultrathin fibers. *Nanotechnology*, *46*, 5670–5703.
5. Pham, Q. P., Sharma, U., & Mikos, A. G. (2006). Electrospinning of polymeric nanofibers for tissue engineering applications: a review. *Tissue Engineering*, *12*(5), 1197–1211.
6. Roshmi, T., Soumya, K. R., Jyothis, M., & Radhakrishnan, E. K. (2015). Electrospun polycaprolactone membrane incorporated with biosynthesized silver nanoparticles as effective wound dressing material. *Applied Biochemistry and Biotechnology*, *176*(8), 2213–2224.
7. Yoshimoto, H., Shin, Y. M., Terai, H., & Vacanti, J. P. (2003). A biodegradable nanofiber scaffold by electrospinning and its potential for bone tissue engineering. *Biomaterials*, *24*, 2077–2082.
8. Agarwal, S., Wendorff, J. H., & Greiner, A. (2010). Chemistry on electrospun polymeric nanofibers: merely routine chemistry or a real challenge. *Macromolecular Rapid Communications*, *31*, 1317–1331.
9. Nitanan, T., Akkaramongkolporn, P., Rojanarata, T., Ngawhirunpat, T., & Opanasopit, P. (2013). Neomycin-loaded poly(styrene sulfonic acid-co-maleic acid) (PSSA-MA)/polyvinyl alcohol (PVA) ion exchange nanofibers for wound dressing materials. *International Journal of Pharmaceutics*, *448*, 71–78.

10. Unnithana, A. R., Barakat, N. A. M., Pichiah, P. B. T., Gnanasekarane, G., Nirmalab, R., Chad, Y.-S., Junge, C. H., El-Newehy, M., & Kim, H. Y. (2012). Wound-dressing materials with antibacterial activity from electrospun polyurethane–dextran nanofiber mats containing ciprofloxacin HCl. *Carbohydrate Polymers*, *90*, 1786–1793.
11. Karami, Z., Rezaeian, I., Zahedi, P., & Abdollahi, M. (2013). Preparation and performance evaluations of electrospun poly( $\epsilon$ -caprolactone), poly(lactic acid), and their hybrid (50/50) nanofibrous mats containing thymol as an herbal drug for effective wound healing. *Applied Polymer Science*, *129*, 756–766.
12. Lin, J., Li, C., Zhao, Y., Hu, J., & Zhang, L. M. (2012). Co-electrospun nanofibrous membranes of collagen and zein for wound healing. *ACS Applied Materials & Interfaces*, *4*, 1050–1057.
13. Merrell, J. G., McLaughlin, S. W., Tie, L., Laurencin, C. T., Chen, A. F., & Nair, L. S. (2009). Curcumin loaded poly( $\epsilon$ -caprolactone) nanofibers: diabetic wound dressing with antioxidant and anti-inflammatory properties. *Clinical and Experimental Pharmacology and Physiology*, *36*, 1149–1156.
14. Jin, G., Prabhakaran, M. P., Kai Dan Annamalai, S. K., Arunachalam, K. D., & Ramakrishna, S. (2013). Tissue engineered plant extracts as nanofibrous wound dressing. *Biomaterials*, *34*, 724–734.
15. Son, B., Yeom, B.-Y., Song, S. H., Lee, C.-S., & Hwang, T. S. (2009). Antibacterial electrospun chitosan/poly(vinyl alcohol) nanofibers containing silver nitrate and titanium dioxide. *Applied Polymer Science*, *111*, 2892–2899.
16. Asran, A. S., Razghandi, K., Aggarwal, N., Michler, G. H., & Groth, T. (2010). Nanofibers from blends of polyvinyl alcohol and polyhydroxy butyrate as potential scaffold material for tissue engineering of skin. *Biomacromolecules*, *11*, 3413–3421.
17. Abdelrahman, M. A., Samuel, M. H., & Orlando, J. R. (2014). Antimicrobial wound dressing nanofiber mats from multicomponent (chitosan/silver-NPs/polyvinyl alcohol) systems. *Carbohydrate Polymers*, *100*, 166–178.
18. Sarhan, W. A., & Azzazy, M. E. (2015). High concentration honey chitosan electrospun nanofibers: biocompatibility and antibacterial effects. *Carbohydrate Polymers*, *122*, 135–143.
19. Moreno, I., González-González, V., & Romero-García, J. (2011). Control release of lactate dehydrogenase encapsulated in poly (vinyl alcohol) nanofibers via electrospinning. *European Polymer Journal*, *47*, 1264–1272.
20. Zulkifli, F. H., Shahitha, F., Yusuff, M. M., Hamidon, N. N., & Chahal, S. (2013). Cross-linking effect on electrospun hydroxyethyl cellulose/poly(vinyl alcohol) nanofibrous scaffolds. *Procedia Engineering*, *53*, 689–695.
21. Schmolka, I. R. (1972). Artificial skin I. Preparation and properties of pluronic F-127 gels for treatment of burns. *Journal of Biomedical Materials Research Part A*, *6*, 571–582.
22. Gombotz, W. R., & Pettit, D. K. (1995). Biodegradable polymers for protein and peptide drug delivery. *Journal of Bioconjugate Chem*, *6*, 332–351.
23. Jushasz, J., Lenaerts, V., Taymond, P., & Ong, H. (1989). Diffusion of rat atrial natriuretic factor in thermoreversible poloxamer gels. *Biomaterials*, *10*, 265–268.
24. Viegas, T.X., Reeve, L.E., and Levinson, R.S. (1994). U.S. Patent, 5,306,501.
25. Viegas, T.X., Reeve, L.E., & Henry, R.L. (1994). U.S. patent, 5,346,703.
26. El-Aassar, M. R. (2013). Functionalized electrospun nanofibers from poly (AN-co-MMA) for enzyme immobilization. *Journal of Molecular Catalysis B: Enzymatic*, *85*, 140–148.
27. El-Aassar, M. R., Al-Deyab, S. S., & Kenawy, E. (2013). Covalent immobilization of  $\beta$ -galactosidase onto electrospun nanofibers of poly (AN-co-MMA) copolymer. *Applied Polymer Science*, *127*, 1873–1884.
28. Wist, J., Sanabria, J., Dierolf, C., Torres, W., & Pulgarin, C. (2004). Evaluation of photocatalytic disinfection of crude water for drinking water production. *Journal of Photochemistry and Photobiology A: Chemistry*, *147*, 241–246.
29. Grassian, V. H., Oshaughnessy, P. T., Adamcakova-Dodd, A., Pettibone, J. M., & Thome, P. S. (2007). Inhalation exposure study of titanium dioxide nanoparticles with a primary particle size of 2 to 5 nm. *Environmental Health Perspectives*, *115*, 397–402.
30. Borenfreund, E., & Puerner, J. A. (1985). Toxicity determined in vitro by morphological alterations and neutral red absorption. *Toxicology Letters*, *24*, 119–124.
31. Bechert, T., Steinrücke, P., & Guggenbichler, J. P. (2000). A new method for screening anti-infective biomaterials. *Journal of Natural Medicines*, *6*, 1053–1056.
32. Kitkulnumchai, Y., Ajavakom, A., & Sukwattanasinitt, M. (2008). Treatment of oxidized cellulose fabric with chitosan and its surface activity towards anionic reactive dyes. *Cellulose*, *15*, 599–608.
33. Thamaphat, K., Limsuwan, P., & Ngotawornchai, B. (2008). Phase characterization of TiO<sub>2</sub> powder by XRD and TEM. *Journal of Natural Sciences*, *42*, 357–361.
34. Shalumon, K. T., Binulal, N. S., Selvamurugan, N., Nair, S. V., Menon, D., & Furuike, T. (2009). Electrospinning of carboxymethyl chitin/poly(vinyl alcohol) nanofibrous scaffolds for tissue engineering applications. *Carbohydrate Polymers*, *77*, 863–869.



35. Cetiner, S., Kalaoglu, F., Karakas, H., & Sarac, A. S. (2010). Electrospun nanofibers of polypyrrole-poly(acrylonitrile-co-vinyl acetate). *Textile Research Journal*, *80*, 1784–1792.
36. Hsu, S. H., Chou, C. W., & Tseng, S. M. (2004). Enhanced thermal and mechanical properties in polyurethane/Au nanocomposites. *Macromolecular Materials and Engineering*, *289*, 1096–1101.
37. Shi, H., Magaye, R., Castranovaand, V., & Zhao, J. (2013). Titanium dioxide nanoparticles: a review of current toxicological data. *Particle and Fiber Toxicology*, *10*, 15.
38. Lee, S., Pereira, B. P., & Yusof, N. (2009). Unconfined compression properties of a porous poly(vinyl alcohol)-chitosan-based hydrogel after hydration. *Acta Biomaterialia*, *5*, 1919–1925.
39. Chuang, W., Young, T., Yao, C., & Chiu, W. (1999). Properties of the poly(vinyl alcohol)/chitosan blend and its effect on the culture of fibroblast in vitro. *Biomaterials*, *20*, 1479–1487.
40. Ramovatar, M., Kumari, K., & Paulraj, R. (2015). Cytotoxic and genotoxic effects of titanium dioxide nanoparticles in testicular cells of male wistar rat. *Applied Biochemistry and Biotechnology*, *175*(2), 825–840.
41. Shah, M. S. A., Nag, M., Kalagara, T., Singh, S., & Manorama, S. V. (2008). Silver on PEG-PU TiO<sub>2</sub> polymer nanocomposite films; an excellent system for antibacterial applications. *Materials Chemistry*, *20*, 2455–2460.
42. Weir, E., Lawlor, A., Whelan, A., & Regan, F. (2008). The use of nanoparticles in anti-microbial materials and their characterization. *Analyst*, *133*, 835–845.
43. Roy, S. C., Varghese, O. K., Paulose, M., & Grimes, C. A. (2010). Toward solar fuels: photocatalytic conversion of carbon dioxide to hydrocarbons. *ACS Nano*, *4*, 1259–1278.
44. Vincent, M. G., John, P. N., Narayanan, P. M., Vani, C., & Sevanan, M. (2014). In vitro study on the efficacy of zinc oxide and titanium dioxide nanoparticles against metallo beta-lactamase and biofilm producing *Pseudomonas aeruginosa*. *Applied Pharmaceutical Science*, *4*, 41–46.
45. Santhoshkumar, T., Rahuman, A., Jayaseelan, G., & Rajakumar, G. (2015). Green synthesis of titanium dioxide nanoparticles using *Psidium guajava* extract and its antibacterial and antioxidant properties. *Asian Pacific Journal of Tropical Medicine*, *7*(12), 968–976.